In Vivo Localization of DNA Sequences and Visualization of Large-Scale Chromatin Organization Using Lac Operator/Repressor Recognition

Carmen C. Robinett,* Aaron Straight,‡ Gang Li,* Carol Willhelm,* Gail Sudlow,* Andrew Murray,‡ and Andrew S. Belmont*

*Department of Cell and Structural Biology, University of Illinois, Urbana-Champaign, Urbana, Illinois 61801; and ‡Department of Physiology, School of Medicine, University of California San Francisco, San Francisco, California 94143-0444

Abstract. We report a new method for in situ localization of DNA sequences that allows excellent preservation of nuclear and chromosomal ultrastructure and direct, in vivo observations. 256 direct repeats of the lac operator were added to vector constructs used for transfection and served as a tag for labeling by lac repressor. This system was first characterized by visualization of chromosome homogeneously staining regions (HSRs) produced by gene amplification using a dihydrofolate reductase (DHFR) expression vector with methotrexate selection. Using electron microscopy, most HSRs showed ~100-nm fibers, as described previously for the bulk, large-scale chromatin organization in these cells, and by light microscopy, distinct, large-scale chromatin fibers could be traced in vivo up to 5 μm in length. Subsequent experiments demonstrated the potential for more general applications of this labeling technology. Single and multiple copies of the integrated vector could be detected in living CHO cells before gene amplification, and detection of a single 256 lac operator repeat and its stability during mitosis was demonstrated by its targeted insertion into budding yeast cells by homologous recombination. In both CHO cells and yeast, use of the green fluorescent protein–lac repressor protein allowed extended, in vivo observations of the operator-tagged chromosomal DNA. Future applications of this technology should facilitate structural, functional, and genetic analysis of chromatin organization, chromosome dynamics, and nuclear architecture.

How chromatin is packaged into higher order structures above the 30-nm chromatin fiber in higher eukaryotic cells and what this level of organization implies for regulation of transcription, DNA replication, and recombination represents a major question in cell biology today. For the mammalian metaphase chromosome, the packing ratio is estimated as 10,000:1, roughly 250 times the 30–40-fold packing ratio measured for the 30-nm higher order chromatin fiber (Alberts et al., 1994). A similar estimate of the packing ratio is more difficult to obtain for interphase chromatids, but several experiments suggest a packing ratio at least an order of magnitude higher than the 30-nm chromatin fiber (Lawrence et al., 1990). The folding motifs accounting for this additional compaction are poorly understood, to a large degree because of the lack of suitable methods for visualization of chromatin structure at this level of organization. In particular, there is a large experimental gap between current electron microscopy approaches to the structure of 30-nm chromatin fibers and the larger-scale chromosome organization analyzed by fluorescence in situ hybridization (FISH),[1] which can only be done on fixed cells after DNA denaturation.

Most investigation has focused on the structure of maximally condensed, metaphase chromosomes. An experimental approach based largely on unfolding chromosome structure through extraction of chromosomal proteins has led to a radial loop model of chromosome structure in which structural proteins, resistant to high salt and detergent extraction, anchor the bases of DNA loops to a central chromosome "scaffold" (Paulson and Laemmli, 1977; Marsden and Laemmli, 1979; Adolph, 1980), which itself may be helically coiled (Rattner and Lin, 1985; Boy de la

Address all correspondence to Dr. Andrew S. Belmont, Department of Cell and Structural Biology, B107 Chemical and Life Sciences Laboratories, 601 S. Goodwin Ave., University of Illinois, Urbana-Champaign, Urbana, IL 61801. Tel.: (217) 244-2311. Fax: (217) 244-1648.

Carmen Robinett's current address is the Department of Cell and Molecular Biology, University of California, Berkeley.

Carol Willhelm's current address is the Southern Illinois Medical School.

1. *Abbreviations used in this paper*: CMF-PBS, calcium-, magnesium-free phosphate-buffered saline; DAPI, 4′,6′-diamidino-2-phenylindole; DHFR, dihydrofolate reductase; FISH, flourescence in situ hybridization; GFP, green fluorescent protein; HSR, homogeneously staining region; MTX, methotrexate; NLS, nuclear localization signal; TEM, transmission electron microscope.

Tour and Laemmli, 1988). Implications of these observations for in vivo chromosome structure have been controversial, though, because of experimental uncertainty regarding the actual nature of DNA organization in such preparations and possible artifacts produced during extraction.

As an alternative approach, we have been examining interphase chromosome structure during cell cycle progression, with the goal of identifying folding intermediates in the pathway of chromosome condensation or decondensation. In earlier work, large-scale chromatin domains, ~100–130 nm in diameter, were visualized in mitotic chromosomes and early G1 interphase nuclei from *Drosophila* and mammalian somatic cells (Belmont et al., 1987, 1989). More recently, serial thin section reconstructions of nuclei from CHO cells were used to demonstrate that these large-scale chromatin domains in fact correspond to actual fibers and therefore represent a distinct level of chromatin folding above the 30-nm chromatin fiber. Chromatid decondensation during G1 was associated with a progressive uncoiling and straightening of this 100–130-nm "chromonema" fiber (Belmont and Bruce, 1994). As cells approached S phase, further chromatin decondensation led to formation of a 60–80-nm chromonema fiber within which folding of 20–30-nm chromatin fibers could be visualized. These chromonema fibers could be traced within the serial sections as distinct fibers for over 2 μm in length. Using similar methods, a similar hierarchy of large-scale chromatin folding has been observed during G2 and prophase chromosome condensation (Li, G., and A.S. Belmont, manuscript submitted for publication).

Together, these results have suggested a folded chromonema model of mitotic and interphase chromosome structure in which topologically complex folding/unfolding of chromonema fibers underlies basic mechanisms of chromosome condensation/decondensation. Evaluating the biological significance of these experimental results, however, will include addressing the following questions: First, do these chromonema fibers exist within living cells? Second, are there reproducible differences in chromatin folding at this level of organization for specific chromosomal loci and for different transcriptional states? Third, what is the actual temporal sequence of condensation and decondensation of these chromonema fibers for a specific chromosome region during the cell cycle, and in particular during mitotic chromosome condensation and before and during DNA replication?

To address these questions, we need the ability to recognize specific chromosome regions without perturbing large-scale chromatin organization on a resolution scale appropriate to our electron microscopy analysis. Ideally, we would also like to be able to selectively visualize these same regions at lower resolution by light microscopy in living cells.

In this paper, we report initial results using a novel method for in situ localization of DNA sequences based on binding of sequence-specific DNA-binding proteins, using the lac operator/repressor as a model system. This method was initially used to visualize, by both light and electron microscopy, chromosome homogeneously staining regions (HSRs) generated by gene amplification. Three methods for repressor staining—exogenous repressor staining of fixed cells, in vivo expression of repressor followed by immunostaining, and in vivo expression of a green fluorescent protein–lac repressor fusion protein—produced similar light microscopy results. In particular, we confirm the organization of chromatin into large-scale chromatin fibers within living cells. Additional work demonstrates the capability of this technique to visualize individual vector insertions in the absence of gene amplification. Using homologous recombination in yeast, it was possible to target specific chromosome sequences for labeling. In both the mammalian and yeast cells, use of a green fluorescent protein (GFP)–lac repressor fusion protein allows direct in vivo visualization of chromosome dynamics.

Materials and Methods

Tissue Culture

CHO cells with a double deletion for the dihydrofolate reductase (DHFR) locus (DG44 CHO cell line [Urlaub et al., 1986]) were grown at 37°C in 5% CO_2 using F12 media with 10% FCS (Hyclone Labs, Logan, UT). After transfection with pSV2-DHFR (see below), stable transformants were selected using F12 media without hypoxanthine and without thymidine (Specialty Media, Lavallette, NJ, or GIBCO BRL, Gaithersburg, MD) and dialyzed FCS (Hyclone Labs). Synchronization in late G1/early S was carried out by blocking cells in G1 using a 36-h incubation in isoleucine-deficient F-10 media with 10% dialyzed FCS (Irvine Sci., Santa Ana, CA), followed by release and a second, S phase block using hydroxyurea (Tobey et al., 1990; Belmont and Bruce, 1994).

Construction of Lac Operator Tandem Repeats

pUC 18 plasmid first was modified to allow a cloning scheme that doubled the number of direct repeats with each cloning cycle. The pUC 18 EcoRI and NarI sites each were eliminated by restriction digest, filling in of 5′ overhangs with the Klenow fragment of *Escherichia coli* DNA polymerase 1, and ligation. The polylinker then was modified to contain SalI-XbaI-NarI-EcoRI-XhoI-BamHI-XmaI-KpnI sites. All cloning steps used the recA minus, *E. coli* host strain, DH5α.

Lac operator tandem repeats were made starting with a lac operator 8-mer sequence (Sasmor and Betz, 1990). This 292-bp lac operator 8-mer sequence, flanked by EcoRI sites, was inserted into the EcoRI site of the modified pUC 18 polylinker. Using SalI, XhoI, and BamHI enzymes, as diagrammed in Fig. 1, doubled the number of direct repeats of the sequence lying between the SalI and XhoI restriction sites with each cloning cycle. This strategy relied on compatible sticky ends generated by SalI and XhoI, which when ligated generated a site that could not be recut with either enzyme. Five rounds of this cloning cycle generated 32 direct repeats of this SalI-XhoI fragment containing the lac operator 8-mer sequence, and therefore generated 256 copies of the lac operator in an ~10.1-kb, "8.32" DNA fragment. With increasing direct repeat copy number, the plasmid became increasingly unstable because of recombination.

Gene Amplification

To carry out gene amplification using DHFR as the selectable marker, the lac operator repeats described above were cloned into the DHFR mammalian expression vector, pSV2-DHFR (Subramani et al., 1981). The EcoRI site in pSV2-DHFR, 3′ of the DHFR cDNA, was replaced with a KpnI-SalI-SphI polylinker. The 8.32 lac operator repeat was force cloned into the modified pSV2-DHFR vector using the KpnI-SalI sites.

DG44 CHO cells were used for $CaPO_4$ transfection (Chen-C. and Okayma-H., 1987) of pSV2-DHFR-8.32. Populations of stable transformants were used for gene amplification. Methotrexate (MTX) concentration was increased in 3–10-fold steps, from 0.02 μM through 100 μM over a period of months. At several MTX concentrations, cells from the pSV2-DHFR-8.32 transfection were subcloned by serial dilution. Alternatively, DG44 CHO cells were transfected using Lipofectamine (Life Technologies, Gaithersburg, MD), or by electroporation under conditions that favored insertion of just one or a few copies of the vector (Boggs et al.,

1986). After electroporation, individual clones were isolated and gene amplification carried out on these clones, as described above.

Southern Blot Analysis

Pulse field gels (1% agarose) were run using the BioRad CHEF II PFGE apparatus (Hercules, CA). 10 μg of genomic DNA was loaded per lane. Mol wt standards included a λ KpnI partial digest, a 1-kb ladder, and linearized pSV2-DHFR-8.32 vector using salmon sperm DNA as a carrier. A mixture of linearized pSV2-DHFR-8.32 vector and λ DNA was used as the probe. The probe was labeled using the Dupont/NEN (Wilmington, DE) Renaissance random primer fluorescein labeling kit and chemoluminescence detection was carried out using the Dupont/NEN CDP-STAR kit.

Modifications and Expression of lac Repressor

We used the p3'SS expression vector to express in CHO cells a lac repressor–nuclear localization signal fusion protein (Fieck et al., 1992). This codes for the wild-type, tetramer lac repressor fused at the carboxyl terminus with a short amino acid linker and the large T antigen nuclear localization signal. We modified this to form a truncated lac repressor that associates as a dimer only and therefore binds to only one lac operator site (Chen and Matthews, 1992); the carboxyl-terminal five amino acids from the lac repressor wild-type sequence were deleted by site-directed mutagenesis.

For expression of a GFP–lac repressor–nuclear localization signal (NLS) fusion protein in yeast, wild-type GFP was cloned into pDK20 (Douglas Kellogg, University of California, Santa Cruz, CA), a plasmid that contains the bidirectional GAL1-GAL10 promoter cloned into pRS306 (Sikorski and Hieter, 1989), by PCR using oligos with overhanging XhoI (5'CGCCTCGAGGAGATGAGTAAAGGAGAAGAACTT3') and EcoRI (5'GCGGAATTCTTTGTATAGTTCATCCATGCC3') sites to yield pGAL-GFP. Oligonucleotides encoding the SV-40 nuclear localization sequence (5'GGGGGATCCTGTACTCCACCAAAGAAGAAGAGAAAGGTTGCCTAATCTAGAGGG3') were inserted into the BamHI and XbaI sites of pGAL-GFP to give an in frame fusion with GFP(pAFS50). The lac repressor was then cloned into the BamHI site of pAFS50 by PCR with oligos containing overhanging BamHI sites (5'CGCGGATCCATGGTGAAACCAGTAACG3', 5'GCGGGATCCCTGCCCGCTTTCCA3') to give pAFS51. Serine 65 of GFP was then mutated to threonine to shift the excitation peak to 495 nm followed by replacement of the KpnI-XhoI GAL promoter fragment with a KpnI-XhoI HIS3 promoter fragment (provided by K. Struhl, Harvard Medical School, Cambridge, MA) to give pAFS67. The carboxyl-terminal 11 amino acids were then deleted from the lac repressor to prevent tetramerization as previously described (Chen and Mattews, 1992) resulting in pAFS78.

To express the GFP–lac repressor–NLS in CHO cells, the XhoI-EcoRV fragment from the yeast vector pAFS51 was ligated into a polylinker and reexcised as an XbaI-EcoRV fragment, which was then inserted into p3'SS. This retains the Kozak sequence from pAFS51 while adding additional restriction sites. This was modified to delete the carboxyl-terminal 5 amino acids of the lac repressor and to mutate serine 65 of GFP to threonine by site-directed mutagenesis.

In Situ Hybridization

A 36-bp single-strand lac operator probe, biotin-labeled at both ends, and fluorescein-labeled avidin were used for detection. For improved chromosome and nuclear morphology, we used formaldehyde fixation while avoiding any steps involving drying of the coverslips (O'Keefe et al., 1992). Cells grown on coverslips were washed in CMF-PBS and then fixed using 2.5% paraformaldehyde in PBS with 5 mM $MgCl_2$ for variable times at room temperature, followed by three 10-min washes in PBS + 300 mM glycine, permeabilization for 5 min in PBS + 0.2% Triton X-100, three 10-min washes in CMF-PBS, and finally incubation in 2× SSC before in situ hybridization.

FISH used a modified procedure derived from two previously described protocols (Trask, 1991; O'Keefe et al., 1992). Denaturation was in 70% formamide, 2× SSC at 80°C for 10 min, followed by 5 min in the same solution on ice and three washes in 2× SSC at room temperature. Hybridization solution consisted of 50% formamide, 2× SSC, 2× Denhardt's solution, 10% dextran sulfate, and 50 mM Tris, pH 7.5, with 2 ng/μl of probe and 1 μg/μl of salmon sperm DNA. 20 μl of hybridization solution was applied per coverslip, and the coverslip was then applied to a glass slide and sealed with rubber cement. Slides were placed in a wet chamber and incubated at 30°C overnight. After incubation, coverslips were washed twice in 50% formamide, 2× SSC at 30°C for 25 min and then twice in 2× SSC at 30°C for 25 min. Hybridization and wash temperatures were determined empirically by optimizing the hybridization signal. Coverslips were then transferred to 4× SSC, blocked with 1% BSA in 4× SSC for 15 min and stained in the same solution with 5 μg/ml FITC-labeled avidin for 2 h at room temperature. Washing of these coverslips used three 5-min changes in 4× SSC, three 5-min changes in 4× SSC + 0.1% Triton X-100, and three 5-min washes in 4× SSC. 2 μg/ml of 4',6'-diamidino-2-phenylindole (DAPI) was used as a DNA counterstain. Coverslips were mounted on glass slides using nail polish.

Lac Repressor Staining of Lac Operator Repeats by Light and Electron Microscopy in CHO Cells

Three methods for light microscopy visualization of lac operators by lac repressor were used. The first used exogenous lac repressor staining after fixation. Cells grown on coverslips were permeabilized for 20 s in PBS* (PBS with 5 mM Mg, 0.1 mM EDTA) + 0.1% Triton X-100, followed by 20 min fixation in 1.6% paraformaldehyde at room temperature in PBS*, and three washes in PBS* with 20 mM glycine. Incubation with 0.06 μM lac repressor in PBS* with 0.1% Triton X-100, 0.1 mM DTT, and 50 μg/ml BSA was followed by a second 15-min paraformaldehyde fixation and immunostaining, as described elsewhere (Belmont et al., 1993), using PBS* buffer throughout. The primary antibody was an anti–lac repressor rabbit IgG (Fiech et al., 1992) and the secondary was a Texas Red–labeled goat anti–rabbit IgG (Jackson ImmunoResearch Labs, Inc., West Grove, PA).

The second method used in vivo lac repressor expression followed by routine immunostaining. Cells were transfected using calcium phosphate (Chen-C. and Okayama-H., 1987) with a eukaryotic expression vector, p3'SS, containing a lac repressor–NLS fusion protein (Fieck et al., 1992). Stable transformants were selected using hygromycin resistance. Cells grown on coverslips were fixed for 3 h at room temperature with 1.6% paraformaldehyde in CMF-PBS, followed by detergent permeabilization and immunostaining, as described above.

The third method used in vivo expression of a GFP–lac repressor–NLS fusion protein, using the NH_2 terminal GFP fusion with the lac repressor/NLS protein encoded by the p3'SS plasmid, described above. Transfection of CHO cells using Lipofectamine (Life Technologies, Gaithersburg, MD) was used to express the fusion protein. Subcloning of stable transformants was used to select clones with suitably high levels of expression of the fusion protein. Visualization was carried out on live cells grown on No. 1 1/2 glass coverslips. For extended observations, cells were grown in a temperature-controlled, FCS2 chamber (Bioptechs, Inc., Butler, PA).

For reasons still unclear, the amount of GFP–repressor–NLS protein expressed was significantly lower, in general, than the wild-type repressor–NLS protein after identical transfection protocols. A small number of cells expressing high levels of the GFP–repressor fusion protein could be found after transient transfection, and in these cells the staining intensity was comparable to the intensity produced by the other methods. In general, expression levels dropped roughly an order of magnitude in the stable transformants. However, significant increases in GFP–repressor levels and fluorescence were produced by growing cells at lower temperatures. Growing cells for 2 d at 32°C increased the percentage of stable transformant cells that showed obvious fluorescence from a few percent to 20–50% in independent transformations of four different amplified cell lines. Cells showing relatively high fluorescence could be cloned and the resulting cell lines had uniform fluorescence levels specific to the particular clone.

Visualization of lac repressor staining by electron microscopy used a modification of the second method described above (Belmont et al., 1993). Cells were grown on Aclar plastic coverslips (Pro-Plastics, Linden, NJ). For visualization of lac repressor staining within intact cells, fixation for 3 h in PBS buffer and immunostaining with primary antibody was identical to the procedure used for light microscopy, but a 1.4-nm gold cluster–labeled secondary antibody (Nanoprobe, Stony Brook, NY) was used in place of the fluorescent-labeled secondary.

After immunostaining, samples were postfixed using 2% glutaraldehyde for 4 h at room temperature. Samples were then washed three times for 5 min in double-deionized H_2O and silver stained (Dancher, 1981). Dehydration, embedding in Epon, sectioning, and uranyl acetate and lead staining of samples were carried out as described previously (Belmont et al., 1993).

For light microscopy, a conventional inverted light microscope (model IMT-2; Olympus Corp., Success, NY) equipped with a Photometrics-cooled (Tucson, AZ), slow-scan CCD camera was used. This system du-

plicates one built by Drs. Agard and Sedat (University of California, San Francisco) and has been described elsewhere (Hiraoka et al., 1991). Briefly, it includes motorized filter wheels for excitation and emission filters (Omega Optical, Brattleboro, VT) and a microstepping motor for z-focus with a Silicon Graphics 4D/35TG computer providing automated data collection using the Resolve3D data collection program (Applied Precision, Mercer Island, WA). A 60×, 1.4 NA Plan Apo oil immersion lens (Olympus Corp.) was used together with narrow pass filters for DAPI, Texas Red, or FITC excitation and emission; GFP images were acquired using the FITC filter combination. Optical sections were collected through entire nuclei at 0.2-μm focal intervals; pixel size was 0.074 μm. Deconvolution of optical sections, to partially restore the image degradation resulting from out-of-focus blur, was accomplished using an enhanced ratio, iterative constrained deconvolution algorithm (Agard et al., 1989).

Thin sections were examined at 100 kV on a transmission electron microscope (model 100C; JEOL USA, Inc., Peabody, MA). Thick sections were viewed using a TEM (model CM200; Phillips Electronic Instrs., Inc., Mahwah, NJ) at 200 kV. An Eikonix (Giesecke & Devriont Engineering, Inc., Bedford, MA) 1412 camera, capable of 12-bit grey scale readout of a 4,096 pixel linear detector array, was used with a Gordon Model 5 × 5 Plannar light source (Gordon Instruments, Orchard Park, NY) to digitize negatives (Belmont et al., 1993).

A "mass normalization" procedure, to convert film optical density values to values proportional to the integrated scattering cross section or electron optical density, was carried out as described previously (Belmont et al., 1987). Image "intensity" values then reflect the density of heavy metal staining, with brighter regions corresponding to higher electron density as in a negative.

The display program, NewVision (Pixton and Belmont, 1996), running on an SGI 4D/35 TG (Silicon Graphics, Mountain View, CA), was used to display images and view results. Selected images or montages were then assembled into figures using Adobe Photoshop. Figures were printed using a Mitsubishi (Tokoyo, Japan) Colorstream printer.

Visualization of Lac Repeats in Yeast

Yeast strain AFS168, expressing the GFP–repressor, was made by integration of pAFS78 into the HIS3 locus of yeast strain AFS34 (W303-1a derivative) after linearization with NheI. The 256 lac operator repeat was introduced into yeast by cloning the KpnI-SphI fragment of pSV2-DHFR-8.32 into the yeast integrating plasmid YIplac128 to yield pAFS59. pAFS59 was linearized with EcoRV, which cuts within LEU2, and transformed into yeast strain AFS168, resulting in strain AFS173. Transformants were selected for leucine prototrophy, and integration at leu2-3,112 was verified by Southern blotting.

A logarithmically growing culture of AFS173 was arrested for 3 h in YPD at 24°C by incubation with 10 μg/ml a-factor. Cells were then washed out of YPD a-factor into CSM-HIS + 10 μg/ml a-factor. Expression of the GFPlacI fusion was induced by adding 3-aminotriazole to 10 mM to the arrested cells for 30 min at 24°C. Cells were then washed into CSM-HIS with or without 15 μg/ml nocodazole and aliquots were put on ice every 10 min for 2 h. Cells were imaged on a microscope (model MicrophotSA; Nikon, Inc., Melville, NY) using a 60× oil immersion lens. Fluorescence was visualized with a conventional FITC excitation filter and a long pass emission filter. Images were acquired with a MTI-SIT68 Camera (Dage-MTI, Inc., Michigan City, IN) using MaxVision-AT software. All images were averages of 128 optical frames of 33 ms each.

Results

Experimental Design

As an alternative to in situ hybridization, we decided to explore use of protein-DNA recognition for localization of specific chromosome sequences within interphase nuclei. To establish this technology, we began this work using gene amplification. Previous characterization of chromosome HSRs produced by gene amplification has shown that they typically contain tens to hundreds of copies of a several hundred- to thousand-kb region surrounding the selectable marker used for amplification (Delidakis et al., 1989). Gene amplification therefore provides an easy way to amplify the number of copies of the DNA sequence used for recognition, thereby increasing the signal to noise ratio for detection while the staining methodology is being developed. Cloning cells at different stages of gene amplification provides a convenient method for preparing different size chromosome segments that can be visualized selectively.

For these initial experiments, we chose the lac operator–repressor system because lac repressor binds to operator with a K_d of 10^{-13}, six orders of magnitude lower than nonspecific binding (Miller and Rezinkoff, 1980), and also has a high affinity for operator sequences located within nucleosomes (Chao et al., 1980). In eukaryotic cells, the lac operator–repressor system has been used to repress transcription (Brown et al., 1987; Hu and Davidson, 1987), and IPTG allows regulation of lac repressor binding in vivo (Fieck et al., 1992).

Fig. 1 summarizes the overall experimental approach used to generate HSRs containing multiple lac operators. A DNA segment containing eight direct repeats of a 36-bp lac operator sequence (Sasmor and Betz, 1990) was cloned between unique SalI and XhoI sites. The compatible sticky ends produced by SalI and XhoI allowed a doubling of direct repeats of the sequence between these two sites with each cloning cycle, as diagrammed in Fig. 1 *A*. Five cloning cycles generated a 256 copy lac operator repeat, which was then inserted into a mammalian DHFR expression vector. Stable transformants were selected using growth in thymidine-free media. Cells having undergone gene amplification were then selected using progressive increases in MTX levels.

Southern dot blot analysis (data not shown) was initially used to confirm the presence of high levels of lac operator repeats in these cells. Screening by FISH, or later by lac repressor staining, was used to select cell clones with chromosomal, versus double minute, gene amplification. Lac repressor staining used three different methods: addition of lac repressor protein to fixed cells followed by immunostaining, in vivo expression of a lac repressor–NLS fusion protein (Fieck et al., 1992) followed by immunostaining, or in vivo expression of a GFP–lac repressor–NLS fusion protein. Initially we used the wild-type lac repressor–NLS fusion protein, but later used site directed mutagenesis to eliminate the COOH terminal five amino acids of the repressor, which are required for tetramer formation (Chen and Matthews, 1992). This mutated protein forms dimers only (Chen and Matthews, 1992), and therefore can form a complex with only a single lac operator. Later experiments, including all of the GFP–repressor results, used this truncated form of the repressor.

Visualization of Chromosome HSRs Containing Lac Operators by Three Methods of Lac Repressor Staining

Initial visualization of lac operator repeats used a particular cell clone, PDC, isolated from a culture that had undergone high levels of gene amplification (up to 100 μM MTX). Repressor staining of metaphase chromosomes showed that these cells contain large amplified chromosome regions, typically ~0.5 μm or longer, corresponding to tens of Mbp in size. Stable transformants of this cell clone, which expressed a wild-type lac repressor–NLS fusion protein

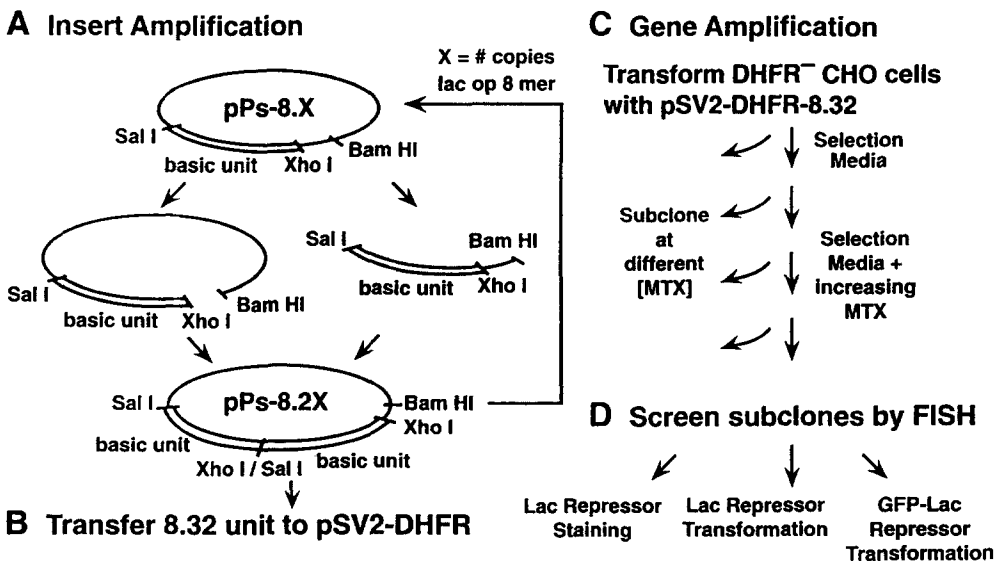

Figure 1. Experimental approach: (*A*) A pUC 18 derivative allowed the generation of 32 copies of a lac operator 8-mer direct repeat. Using SalI, XhoI, and BamHI enzymes, as diagrammed above, doubled the repeat number with each cloning cycle. (*B*) DHFR⁻ CHO cells (DG44) were stably transformed with a DHFR expression vector, pSV2-DHFR, containing this 256 copy lac operator repeat. (*C*) MTX concentration was increased in 3–10-fold steps, from 0.02 μM through 100 μM MTX. (*D*) Initial screening by FISH selected cell clones with chromosomal, versus double minute, gene amplification. Lac repressor staining used either of three methods: addition of lac repressor protein to fixed cells followed by immunostaining, in vivo expression of a lac repressor–NLS fusion protein and immunostaining, or direct visualization of a GFP–lac repressor–nuclear localization signal fusion protein.

(Fieck et al., 1992), were used in these experiments. Fig. 2 shows a representative field, after deconvolution, containing several cells stained using a primary, anti-lac repressor primary antibody after formaldehyde fixation.

The signal intensity with the repressor immunolocalization was quite high. A direct comparison with the signal intensity after FISH was not done since we used different fluorochromes for detection. However, typical exposure times with our CCD camera for indirect immunofluorescence localization of lac repressor staining were 0.05–0.2-s (Texas Red) versus 5–10-s typical exposures for FISH using FITC-labeled avidin. For comparison, these 0.05–0.2-s exposures were severalfold to more than 10× shorter than typical exposure times used for indirect immunofluorescence using anti–lamin B or vimentin primary antibodies with the same filter sets and imaging system.

Many nuclei show multiple HSRs in these highly amplified cultures. As expected from previous FISH studies of interphase chromosome structure, regions of staining corresponded to compact domains just several microns in size (Manuelidas, 1985; Trask, 1991; Cremer et al., 1993). Fig. 2, however, also reveals a prominent substructure within these HSR domains, suggestive of a fibrillar packing, which was not obvious in previous FISH results. At the edges of these compact regions, individual fibers can be recognized whose 0.2–0.3 μm widths are similar to the expected, diffraction-limited widths measured previously for chromonema fibers by DAPI staining (Belmont et al., 1989; Belmont and Bruce, 1994).

Two experimental concerns led us to develop alternative staining methods. First, we questioned whether the large numbers of lac operator repeats, when bound to lac repressor, would fold normally within interphase and mitotic chromosomes. We therefore were interested in being able to stain fixed cells, which did not express lac repressor, with purified, exogenous lac repressor so that we could compare the morphology of these HSRs with and without in vivo expression of the repressor. Second, we were interested ultimately in being able to visualize chromosome conformation and dynamics in vivo, and to verify that our fixation and staining procedures did not perturb the HSR morphology. Therefore, we explored the use of a GFP–lac repressor fusion protein for in vivo visualization.

Fig. 3 compares lac repressor staining of the HSRs from PDC cells using all three of these methods: immunofluorescence staining of cells that express lac repressor as shown in Fig. 2, exogenous lac repressor staining of fixed PDC cells followed by immunostaining, and direct, in vivo visualization of PDC cells stably transformed with a GFP–lac repressor–NLS fusion protein construct. To improve the intensity of the GFP–repressor signal, we used a single amino acid mutation in the GFP, Ser65 → Thr, described previously (Helm et al., 1995). To avoid questions of differential image enhancement or filtering created by the deconvolution process, in this figure we show the raw images recorded from the CCD camera. (Comparison of Fig. 2 and Fig. 3 *B*, *top*, allows a direct comparison of the original and deconvolved images of the same nucleus.) We note that because the lac repressor staining is localized to only small, local chromosome regions, out-of-focus blur is significantly less of a problem in the raw images relative to the visualization of general chromosomal staining by DAPI.

All three methods yield similar HSR morphologies as viewed by light microscopy. In particular, the fibrillar substructure of the HSRs is prominent with all staining methods, including in vivo observation. Because these results are similar independently of whether the cells express lac repressor, this substructure is not a result of an unusual chromatin conformation induced after in vivo lac repressor expression. Because the GFP–repressor in vivo imaging shows similar results to immunostaining of cells expressing the repressor, this substructure is not an artifact of the immunostaining procedure.

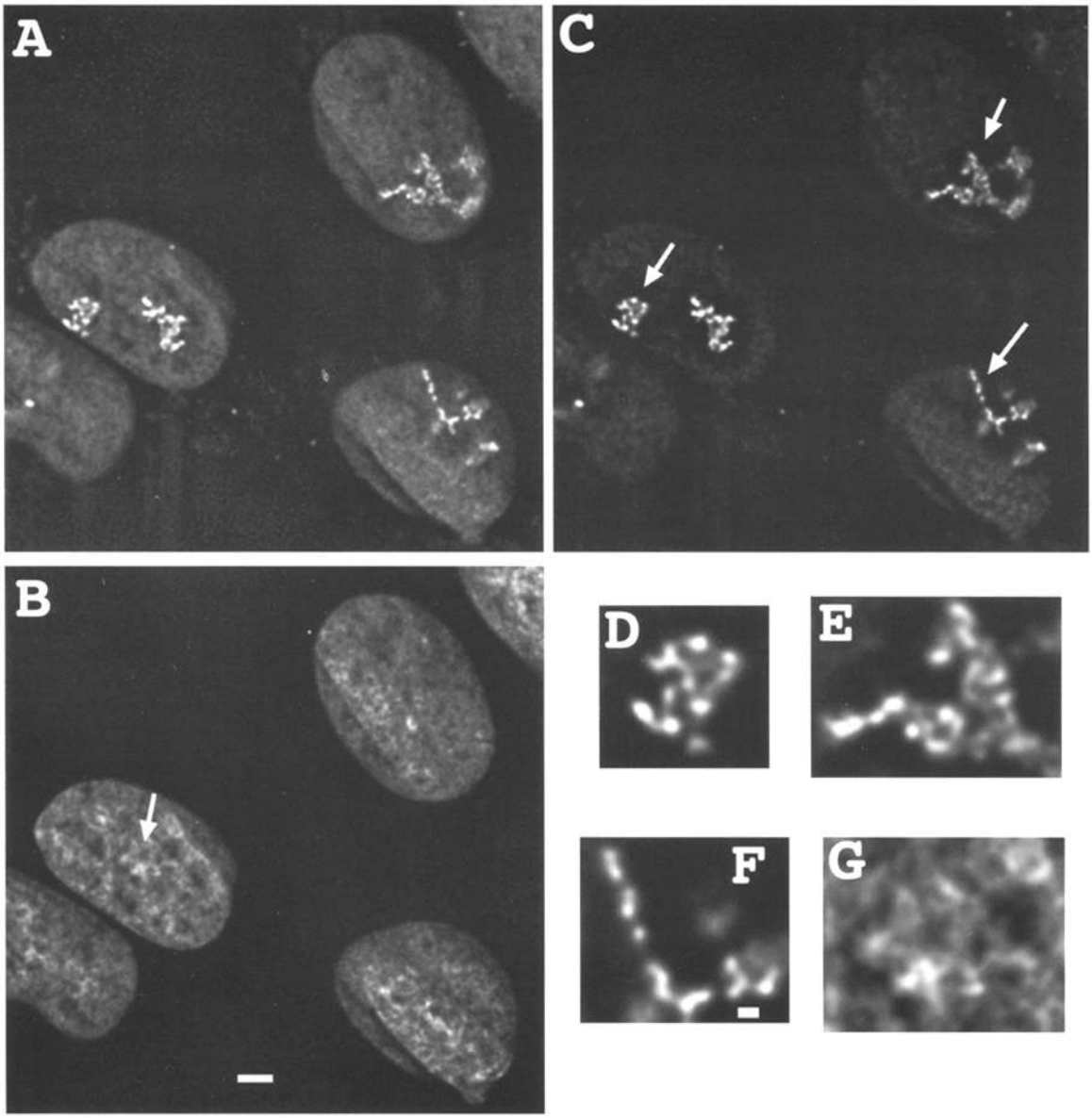

Figure 2. Fibrillar lac repressor staining of amplified chromosome regions within interphase nuclei. Cells selected at 100 μM MTX and expressing the lac repressor–NLS fusion protein were fixed and stained by indirect immunofluorescence with an anti–lac repressor primary antibody. Majority of nuclei show what appear to be compact domains formed by tightly folded fibers. In some nuclei, segments of extended fibers can be visualized in addition to folded regions. A high power field showing several nuclei is shown after optical sectioning and deconvolution; a single optical section is displayed. (*A*) Combined DAPI and immunofluorescence signal. (*B*) DAPI staining alone. (*C*) Lac repressor staining alone. (*D–F*) 3× enlargement of repressor stained regions marked by arrows in *C*. (*G*) 3× enlargement of DAPI stained region marked by arrow in *B*. Bars: (*A–C*) 2 μm; (*D–G*) 0.4 μm.

All three staining methods yield intense and reproducible staining. Typically, the staining of fixed specimens with exogenous lac repressor is roughly comparable in intensity with immunostaining of specimens that express lac repressor in vivo. The intensity produced by the GFP–repressor binding appears to be limited primarily by the expression levels of the fusion protein. In cells with high levels of GFP–repressor expression, as estimated by the level of nuclear background fluorescence, the intensity of the HSR staining is close to that obtained by antibody staining. However, in cells with low levels of GFP–repressor expression, as estimated by low levels of nuclear background fluorescence, the intensity of the HSR staining can be 10–100-fold lower than that obtained by antibody staining. Our experience to date suggests that despite the generally weaker signal, the highest sensitivity is achieved using in vivo expression of the GFP–repressor–NLS fusion protein. This is because the nuclear background staining in these cells usually is extremely low because of lower expression levels of the fusion protein, resulting in a high signal to noise ratio for specific lac operator staining.

Detection of Single 256 Copy Lac Operator Repeat without Prior Gene Amplification

The signal generated by lac repressor staining of the chro-

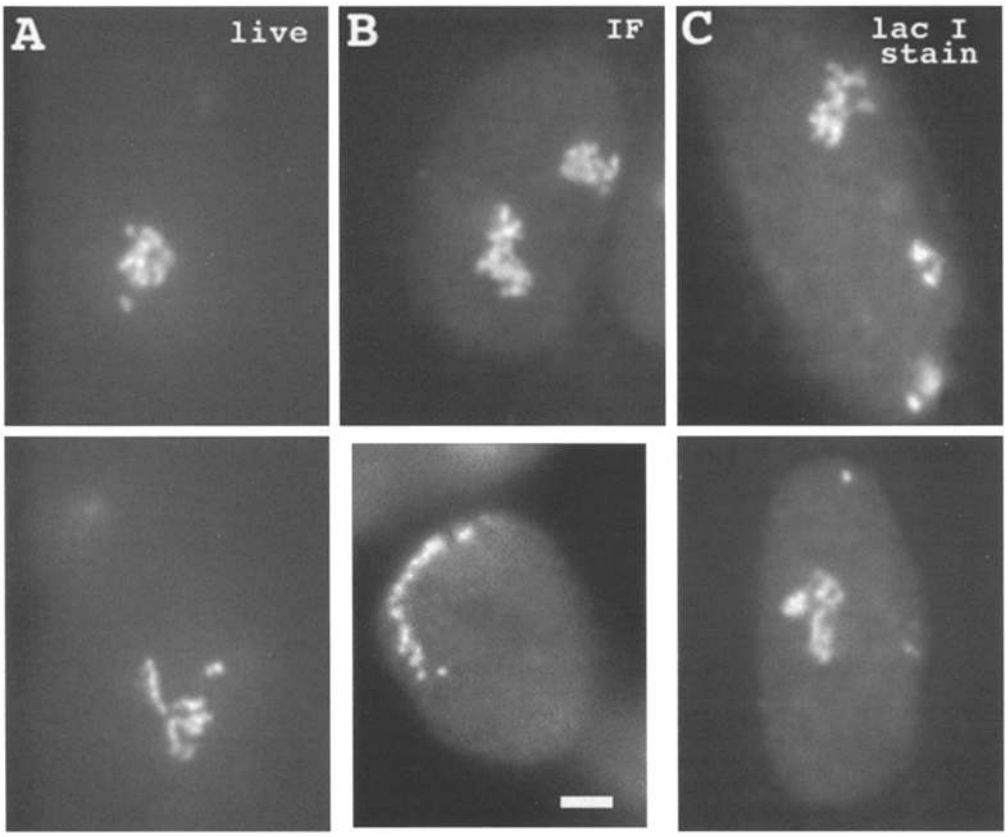

Figure 3. Three methods for lac repressor staining yield similar results. PDC cells selected at 100 μm MTX were stained with three different methods. (*A*) Cells stably expressing a GFP–lac repressor–NLS fusion protein were imaged live in culture media. (*B*) Cells stably expressing a lac repressor–NLS fusion protein were fixed and then stained by indirect immunofluorescence using an anti–lac repressor primary antibody. (*C*) Cells not expressing lac repressor were fixed, stained with purified lac repressor, and then stained by indirect immunofluorescence using an anti–lac repressor primary antibody. The top panel shows the typical HSR appearance, suggestive of coiled fibers within a compact domain. The bottom panel shows examples of cells in which extended fibers can be visualized and traced over large distances. The similar staining patterns seen in *A–C* indicate that the HSR large-scale chromatin conformation is not altered, at light microscopy resolution, by in vivo lac repressor expression, or by fixation and staining procedures. Bar, 2 μm.

mosome HSRs produced by gene amplification was very bright. In cells selected at high amplification levels, corresponding to 100 μM MTX, typical exposure times varied from 0.05–0.2 s for saturation of the CCD camera. These exposure times were essentially the same for two clones isolated at much lower level of amplification, corresponding to 0.3 μM MTX. Presumably this reflects a similar high density of lac operator sites with primarily the size of the HSR varying at different amplification levels.

These results raised the obvious question of how many copies of the 256 lac operator repeat are required for detection, and whether this general approach to in situ localization of DNA sequences could be applied in the absence of gene amplification.

Initial results demonstrated that integration of multiple vector copies in the absence of gene amplification could be easily detected. Cells stably transformed using a Lipofectamine transfection procedure revealed ~50% of stable transformants with obvious lac repressor staining, in the case of exogenous lac repressor staining; this transfection method typically produces tens of vector copies integrated at individual sites. The majority of these cells, ~50–70%, showed single spots of lac repressor staining whose size roughly corresponded to the diffraction limit of resolution of the light microscope (data not shown). However, the intensity of these spots varied significantly, with exposure times for the CCD camera ranging from less than 0.05 s to more than several seconds to obtain equivalent grey scale values. Small clusters of neighboring cells could be recognized that showed similar staining patterns and exposure values, implying that the variations in staining were clonal. For these reasons, the variable signal intensity is likely to correspond primarily to copy number of the vector sequence in the chromosomal insertion.

To provide a better estimate of the detection sensitivity, we next attempted to visualize repressor staining of a specific stable clone, EP1-4, produced by electroporation transfection of the pSV2-DHFR-8.32 plasmid under conditions that favor single or low copy insertions of the vector (Boggs et al., 1986). Initial experiments using exogenous lac repressor staining did not reveal clear staining of the cell clone. We reasoned that our detection efficiency was limited by the background produced by our lac repressor staining. We therefore next attempted to visualize GFP–repressor staining of these cells after transformation with the GFP–repressor vector.

EP1-4 cells stably expressing levels of GFP–repressor sufficient to produce a detectable but low nuclear background were selected for optical sectioning. The low level of fluorescence in these cells and the limited depth of fo-

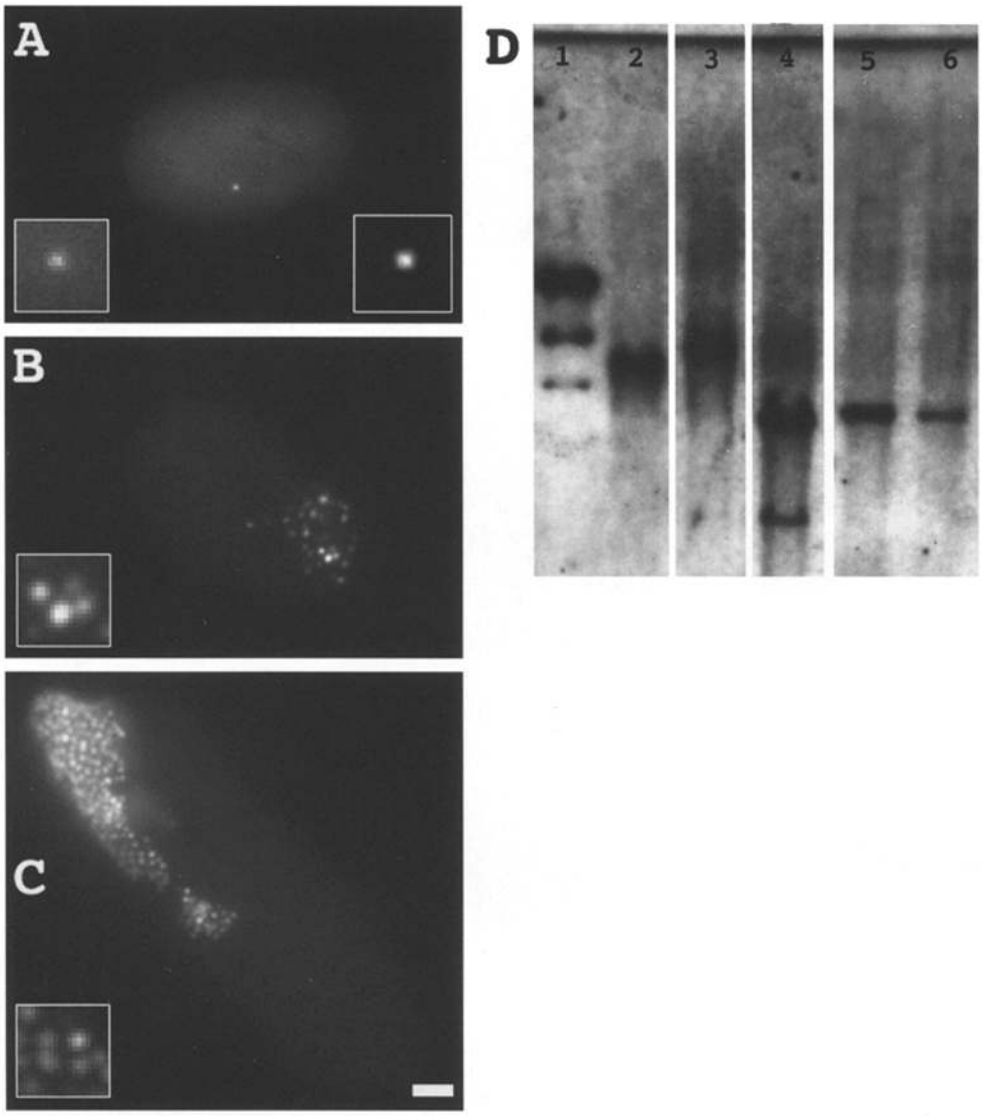

Figure 4. Sensitivity of lac op/repressor staining allows detection of individual copies of integrated vector. *A–C* show in vivo expression of the GFP–lac repressor fusion protein in EP1-4 cells before (*A*) and after gene amplification to 0.5 μM MTX (*B*) and 5 μM MTX (*C*). Left inset in *A* shows single spot of repressor staining from original image; right hand inset in *A* shows same region after background subtraction and contrast enhancement. Gene amplification results in multiple copies of the chromosome region surrounding the original integration site leading to an array of similar intensity spots. (*D*) Southern blot shows vector insert in these cells is single copy. Lane *1*: λ molecular weight standards (partial KpnI digest) at 48.5, 29.9, and 17 kb. Lanes *2* and *3*: EP1-4 genomic DNA digested with BstEII (lane *2*) or DrdI (lane *3*); both are frequent cutters with no sites within the transfected vector. Bands for both digests are less than twice the 15.1-kb vector size. Lane *4*: Ep1-4 genomic DNA digested with ApaI, a unique frequent cutter of the transfected vector. Two bands only are seen as expected for a single copy vector insertion (see text). Lanes *5* and *6*: 11 pg (or ~0.5 copy per genome equivalent) (lane *5*) or 3 pg (lane *6*) of linearized pSV2-DHFR-8.32 vector (15.1 kb). Bar, 2 μm.

cus prevented easy detection of discrete staining, and these cells were chosen solely on the basis of the background nuclear fluorescence. However, in each of seven separate cases, complete optical sectioning revealed exactly one clearly distinguishable spot per nucleus, using relatively long integration times of 5–10 s with our CCD camera. An example of this staining is shown in Fig. 4 *A*.

As a further check to determine that these spots corresponded to real staining of lac operator repeats, this EP1-4 clonal cell line was subjected to several rounds of gene amplification. Fig. 4, *B* and *C*, shows examples of GFP–repressor fluorescence staining in cells from two different stages of this gene amplification. As demonstrated in this figure, staining of chromosome HSRs produced by this amplification now reveals a collection of individual spots. These spots are of similar intensity to the single spot visualized in the original EP1-4 clone before gene amplification. We interpret these spots as sites of pSV2-DHFR-8.32 vector insert(s) within the repeating units produced by gene amplification.

Southern blot analysis determined that the vector insert in these EP1-4 cells was single copy, based on two different criteria. Genomic DNA was cut using two different 6-bp recognition restriction enzymes not present in the pSV2-DHFR-8.32 plasmid, therefore excising the complete vector array plus some amount of flanking DNA. Fig. 4 *D*, lanes *2* and *3*, shows both enzymes produced single bands whose size fell between the 17-and 30-kb size markers (lower two bands, lane *1*), and therefore less than twice the 15.1-kb size of the transfected vector. In addition, digestion with an enzyme with a unique site within the transfected vector produced two bands only, as expected for a single copy insertion, as shown in lane *4*; each band was larger (~5.5 kb and 11–15 kb, as determined by a 1-kb lad-

der mol wt standard [data not shown]), as expected, than the corresponding fragment size produced by the same digest with the SalI linearized vector used for transformation (4.5 and 10.6 kb). Therefore, our detection sensitivity in a mammalian genome allows detection of single copies of the 256 lac operator repeat.

The detection sensitivity appears to be primarily limited by the variability, or "noise," in the nuclear background level. Subtracting out the relatively uniform nuclear background signal, using a local contrast enhancement algorithm (Peii et al., 1982; Belmont et al., 1987), yields a very clear signal for the lac operator/repressor staining, as shown in the right hand inset of Fig. 4 *A*. We estimate that the signal to noise ratio for this spot, as defined by the peak brightness of the spot relative to the intensity variations in the nuclear background staining, is ~12:1.

The nuclear background level of GFP–lac repressor staining is determined by the level of GFP–repressor expression together with the amount of nonspecific DNA binding. A reduction in the genome size, and therefore the amount of nonspecific DNA, should reduce the attainable background level. We therefore expect this detection sensitivity to carry over to cells from other species whose genome size is equivalent or smaller than CHO cells.

HSRs with Distinctive Variations in Large-Scale Chromatin Organization Can Be Isolated

One goal of our work was to be able to construct model chromosome regions whose cell cycle dynamics could be more easily analyzed than bulk chromatin. Our results to date suggest that these chromosome HSRs not only show similar morphology to normal chromosomes but also can reproduce, in different HSRs, the heterogeneity of chromosome condensation observed normally for different chromosome regions.

The most prevalent HSR morphology we have observed to date is the irregular, tightly folded appearance shown in Figs. 2 and 3, top. As discussed above, this appearance is suggestive of a fibrillar substructure with diameter less than or equal to the ~0.2 μm diffraction resolution limit of the light microscopy. Based on previous serial thin section reconstructions of CHO G1 nuclei, this compactly folded fiber appearance is what we would expect for the irregular folding of chromonema fibers in a typical genomic region (Belmont and Bruce, 1994).

Of the ~12 cell clones isolated after gene amplification, most show this morphology for their HSRs. However, we have also identified several clones with distinct HSR morphologies either more or less condensed than the average morphology.

Fig. 5, *A–C*, shows staining of the A03 clone isolated at 0.3 μM MTX selection after amplification of a population of stable transformants produced by calcium phosphate transformation. A low power survey micrograph demonstrates a single, dense staining spot in most cells (Fig. 5 *A*); a few cells have paired spots, representing sister chromatids. Both the size, ~80 Mbp as estimated from its ~1.2-μm length in metaphase chromosomes, and the chromosome location of this HSR are highly stable (Li, G., C. Robinett, G. Sudlow, C. Willhelm, and A.S. Belmont, manuscript in preparation). Based on preliminary experiments, the HSR

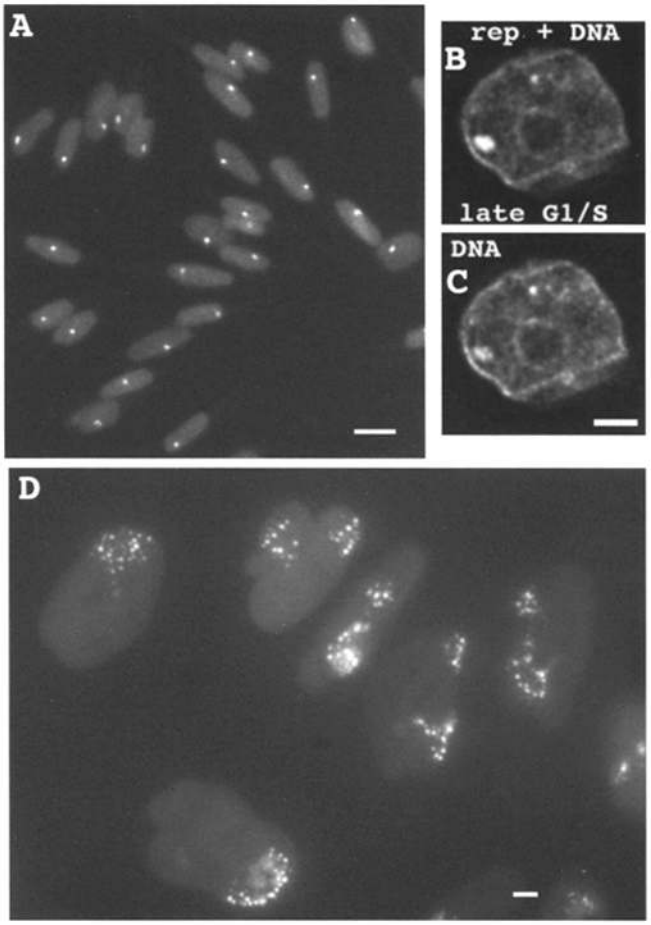

Figure 5. HSRs with distinctive folding patterns can be isolated. A03 clone, isolated at low MTX selection, contains a single, stable, late replicating HSR. (*A*) Low power survey—all nuclei contain a single spot, or a closely spaced doublet, of lac repressor staining. Cells blocked with HU at late G1/early S show a highly condensed HSR that can be localized by repressor staining or even by DAPI staining alone. (*B*) Composite image of DNA and repressor staining. (*C*) DNA (DAPI) staining only. At this cell cycle stage, little substructure is evident and the compaction is comparable to that observed for this HSR in mitotic chromosomes (data not shown). In contrast, EP1-4 cells after gene amplification at 0.5 μM MTX selection show an extended morphology with a much higher frequency of extended fibers than seen in the typical HSR with a tight coiled fiber morphology (see Figs. 2 and 3 and text). Bars: (*A*) 10 μm; (*B–D*) 2 μm.

in this A03 clone behaves as late replicating, heterochromatin (Li, G., C. Robinett, G. Sudlow, C. Willhelm, and A.S. Belmont, manuscript in preparation).

A03 cells blocked in late G1/early S phase show predominately a condensed staining region ~0.5–1.0 μm in diameter, with the percentage of cells with this pattern, 85%, close to the typical percentage of cells with 2c DNA content using this synchronization procedure. Moreover, the size of this region is similar to its size in metaphase chromosomes. An example of this staining is shown in Fig. 5, *B* and *C*. In contrast to typical HSR morphology, showing a fibrillar substructure by light microscopy, this A03 HSR instead appears at light microscopy resolution as a solid density. At this cell cycle stage, most of the chroma-

tin is highly dispersed (Belmont and Bruce, 1994); in contrast, the A03 HSR appears as a condensed mass easily distinguished even in the DAPI-stained image.

Fig. 5 *D* instead shows staining of extended HSRs in a representative, high-power field of cells from a cell clone isolated after gene amplification of EP1-4 cells (see previous section, Fig. 4) up to a 0.5 μM MTX concentration. We speculate that this extended staining pattern may be related to integration of the vector into an "active" chromosomal region capable of permitting significant transcription from the single copy DHFR gene. Subsequent gene amplification would coamplify hundreds of kb of flanking DNA from this region.

Examples of Biological Applications of lac Operator–Repressor Staining

1. Visualization of Chromatin Structure Under Nonperturbing Conditions Supports Existence of Large-Scale Chromatin Fibrillar Structures. As described previously, the typical staining pattern for PDC cells showed compact regions of staining with substructure suggestive of folding of a fibrillar structure. However, the limited resolution of light microscopy, particularly along the z-axis, prevents a definite resolution of actual fibers. In contrast, several examples in which extended, linear fibrillar staining can be traced for ~5 μm in length are shown in the bottom panel of Fig. 3. In these cases, optical sectioning demonstrates that these are in fact extended, continuous fibers (data not shown). Examples of such fibers are shown for all three staining methods, including in vivo observation of the GFP–repressor–tagged HSRs. Given the large size of the HSRs found in these cells, estimated as tens of Mbp or larger from the ~0.5 μm or larger HSR lengths in mitotic chromosomes (for example, see Fig. 7 *E*), the inferred fiber lengths observed in interphase nuclei implies packing ratios of hundreds to thousands to one, well above the estimated 40:1 packing ratio of 30-nm chromatin fibers. Here we define the packing ratio as the ratio of the length of the chromatin fiber to the extended length of the B form DNA within these fibers.

The extended fibers visualized in PDC clones corresponded to relatively infrequent observations appearing in <5% of cells. In contrast, in EP1-4 cells after gene amplification, a high frequency of cells show extended in vivo staining, including examples of linear arrays of spots, in Fig. 5 *D*. We interpret these linear arrays as resulting from a contiguous chromosomal DNA segment, formed from multiple copies of the gene amplification unit, packaged into an extended, linear fiber. The individual spots correspond to the lac operator repeat adjacent to the inserted DHFR gene, with the separation between spots corresponding to the chromosomal flanking DNA within the amplification unit. Assuming that the size of these amplified units is in the usual several hundred to thousand-kb range observed for gene amplification (Delidakis et al., 1989), the observed separation between these spots again suggests packing ratios for these large-scale chromatin fibers of hundreds to one.

2. Comparison of Lac Repressor Staining with Conventional In Situ Hybridization Methods. These results suggestive of the higher order organization of chromatin into spatially distinct, large-scale chromatin fibers are consistent with our previous electron microscopy studies of interphase chromosome structure, as discussed in the introduction. However, the existence of such large-scale chromatin fibers has not generally been appreciated from previous in situ hybridization studies of interphase chromosome organization.

To reconcile our results with previous FISH results, we therefore compared our lac operator/repressor staining with conventional FISH staining using a biotin-labeled, lac operator oligonucleotide probe. PDC cells, selected at high levels of gene amplification (100 μM MTX), were grown directly on the coverslip and fixed after a brief wash in phosphate saline. To roughly assay the extent of perturbation of nuclear and chromosome structure associated with the FISH procedure, we used light microscopy of DAPI-stained mitotic and interphase cells.

Initial experiments revealed pronounced structural perturbations induced by the DNA denaturation step of the hybridization procedure. This was particularly true for cells fixed with methanol (data not shown). Progressive improvement in ultrastructure after DNA denaturation was seen with increases in the time of formaldehyde fixation from 10 min up to 4 h. However, the strength of the FISH signal dropped ~50% with an increase from 3 to 4 h of fixation time in formaldehyde. We therefore chose 3 h of fixation for our experiments.

Fig. 6, *A* and *B*, shows FISH results obtained using these fixation conditions. Consistent with the prior repressor staining results for these cells shown in Figs. 2 and 3, most nuclei showed two to three compact domains of hybridization. Unlike the repressor staining results, however, little substructure was visualized within these domains; the fibrillar substructure apparent by repressor staining was not obvious in the FISH results. In a small percentage of nuclei, extended linear staining regions were seen; two of the better examples we recorded are shown in this figure. However, these linear regions of hybridization appeared more diffuse than we had observed with the repressor staining.

To better describe the changes in ultrastructure induced by a standard FISH protocol, we carried out a comparison of HSR morphology observed in vivo using the GFP–repressor staining versus that seen in the exact same cells after fixation and DNA denaturation. Cells were grown on gridded coverslips and photographed live. They were then fixed for 3 h in formaldehyde and processed up through the DNA denaturation step according to the same protocol used in our previous FISH experiments. Detection of the HSR after DNA denaturation used immunofluorescence staining against the lac repressor rather than in situ hybridization because of the greater signal strength and reliability of repressor staining.

Fig. 6, *C* and *D*, shows the images from a specific nucleus in vivo (*C*) versus after fixation and DNA denaturation (*D*). This nucleus was chosen because the HSR contained a mixture of extended fiber regions and compact domains. Overall the size and shape of the HSR staining is maintained quite well through the mock in situ hybridization protocol. This experiment therefore validates the use of FISH to study the intranuclear distribution of specific chromosome regions and gene loci.

However, there is a noticeable blurring of the fine struc-

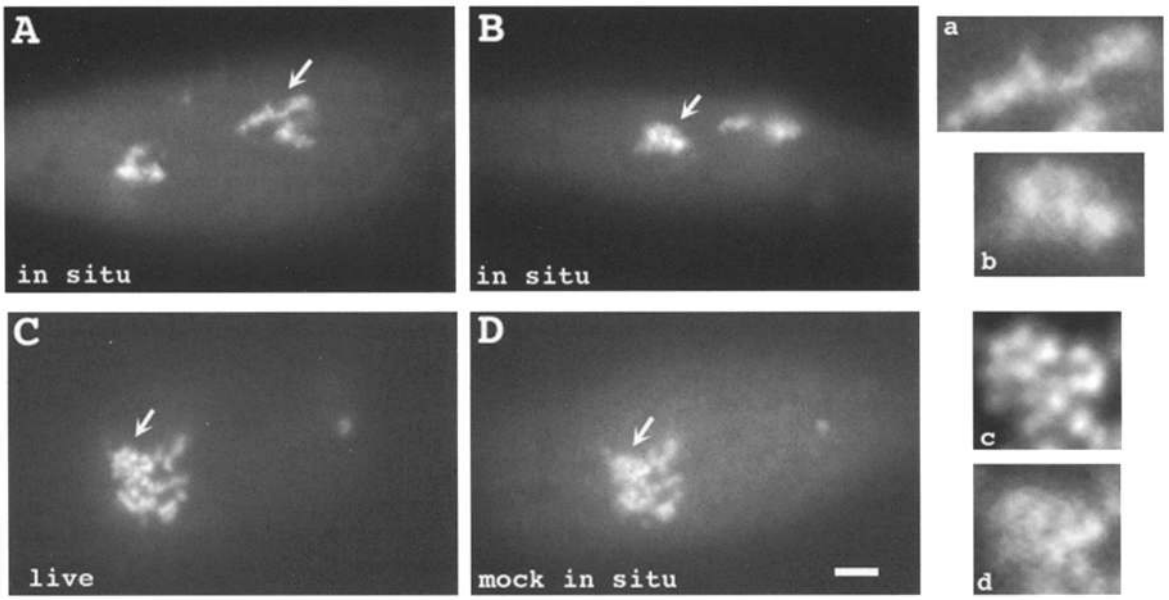

Figure 6. Comparison of HSR morphology in PDC cells visualized in vivo using GFP-repressor expression versus after FISH or DNA denaturation procedures. (*A* and *B*) FISH using extended formaldehyde fixation. Arrows point to regions which are shown at 3× enlargement in *a* and *b*. Compact regions show only hints of substructure (see *arrow* in *B*, *b*), which are obvious with lac repressor staining (Figs. 2 and 3). (*C*) In vivo visualization of HSR with compact regions and extended, linear fibers. (*D*) Immunostaining with anti–lac repressor antibody of same cell as in *C* after a mock in situ hybridization procedure. Arrow (*C* and *D*) points to compact region in which fibrillar substructure is evident in vivo (*C*) but is largely lost after DNA denaturation procedure (*D*) (see also *c* and *d*, 3× enlargement). Bar: (*A–D*) 2 μm.

ture within the HSR; in particular, within the compact regions (marked by *arrows*) of the HSR, the substructure that is obvious within the live image is blurred within the mock in situ image. This is better seen in the enlarged insets of Fig. 6, *c* and *d*, which show the compact regions marked by arrows in the main figure. The blurred appearance of the HSR after the DNA denaturation procedure resembles the actual FISH results shown in *A* and *B*. This blurring is not a focus problem. To ensure comparison of the appropriate focal planes, optical sectioning in 0.2-μm intervals was performed on nuclei after DNA denaturation and repressor staining. The optical section showing the closest similarity to the original live image was selected for comparison.

We therefore conclude that previous lack of appreciation of the fibrillar nature of large-scale chromatin organization from FISH studies may be related to blurring of fibrillar substructure after typical FISH protocols (see Discussion). Although regions of extended staining still appear fibrillar, the compact regions lose obvious fibrillar substructure.

3. Extension of Lac Operator–Repressor Detection to TEM Localization—Further Support for Large-Scale Chromatin Fibrillar Organization. Using immunogold localization, lac repressor staining could also be used for visualization of the amplified chromosome regions by TEM. Immunogold staining was very similar to the immunofluorescence protocols described above, with a 1-nm Nanoprobe gold-labeled secondary antibody replacing the fluorochrome-labeled secondary. As with the immunofluorescence experiments, staining was accomplished either by expressing the repressor–NLS fusion protein in vivo followed by traditional preembedding immunostaining or by staining fixed cells with purified wild-type repressor followed by a second fixation and preembedding immunostaining (data not shown).

Fig. 7, *A* and *B*, shows results from staining nonextracted PDC cells that express the repressor. Cells were fixed 3 h with formaldehyde before detergent treatment and antibody staining, and postfixed in glutaraldehyde for several hours before silver enhancement and embedding. The corresponding immunofluorescence and GFP images for these cells was shown in Fig. 2.

As described earlier, the HSRs in these cells formed domains typically measuring ~2 μm in width and by light microscopy gave the appearance of being formed by tight folding of a fibrillar component. Fig. 7 *A* shows a nuclear cross-section at low magnification from a 0.2-μm Epon section through one of these HSR domains; Fig. 7 *B* shows a higher magnification view containing the HSR. Immunogold staining is intense and reveals short, linear segments of ~80–130-nm diameter labeled by the immunogold staining. Comparably sized regions of heavy uranyl and lead staining nearby the immunogold-labeled HSR are marked by arrows. Fig. 7, *C* and *D*, shows nuclear cross-sections from thicker, 0.5-μm Epon sections; the large-scale fibrillar chromatin structure underlying the HSR staining is now more apparent because of the inclusion of folded fiber lengths within the thicker section. Fig. 7 *F* shows an enlarged region from a 0.5-μm section through an HSR, again revealing segments of ~130-nm fibers. An example of mitotic staining of the HSR is shown in Fig. 7 *E*; an ~0.5 μm chromosome arm segment labeled by immunogold staining is contained within a 0.5-μm thick section.

Previous work using correlative light and electron microscopy (Belmont et al., 1989) has shown that the more in-

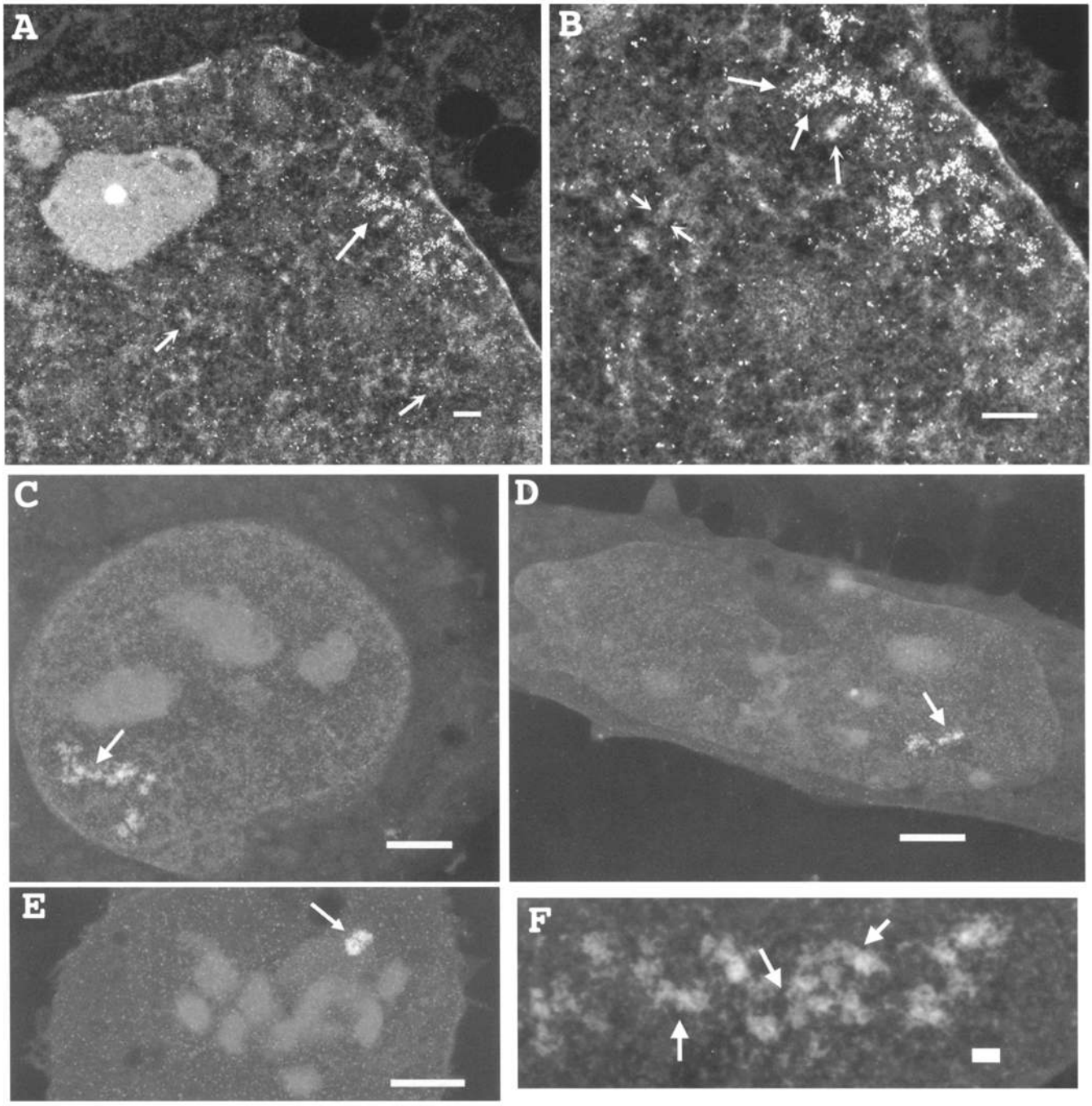

Figure 7. Preembedding immunogold electron microscopy localization of lac repressor staining demonstrates ~100-nm diameter fiberlike segments within nonextracted cells. Cells selected at 100 μM MTX and expressing the lac repressor–NLS fusion protein were fixed for 3 h in formaldehyde and then immunostained before glutaraldehyde fixation and embedding. Intensity is scaled as negative; whiter regions correspond to heavier staining: (*A*) 0.2-μm thick section, low magnification survey; (*B*) twofold higher magnification of lac repressor stained region from *A*. Straight arrowheads point to fiberlike segments of immunogold staining. Concave arrowheads point to similar, uranyl-lead–stained segments of chromonema fibers recognizable above the nucleoplasmic background and distributed throughout the nucleus. (Contrast has been highly enhanced, preventing visualization of the cytoplasm, to allow visualization of these features.) (*C* and *D*) 0.5-μm sections show longer, more extended fiber segments (*arrows*). (Normal contrast levels now allow visualization of cytoplasm and nucleoplasmic background staining.) (*E*) 0.5-μm section through mitotic plate showing labeling of HSR. Arrow points to possible division between sister chromatids. Length of HSR within this section is ~0.5 μm. (*F*) Enlarged example of distinct fiber segments, ~130-nm diameter, within 0.5-μm section through HSR. Bars: (*A* and *B*) 0.5 μm; (*C–E*) 2.0 μm; (*F*) 250 × 120 nm.

tensely, heavy metal–stained regions, as marked by arrows in Fig. 7 *B*, correspond to large-scale chromatin domains, or chromonema fibers, which stain with DAPI. However, visualization of these large-scale domains by TEM is difficult because of the heavily uranyl- and lead-stained nucleoplasmic background. Using cells extracted with detergent in polyamine or divalent cation–containing buffers, we have been able to more easily visualize these large-scale chromatin domains and trace them in three-dimensional reconstructions as extended fibers over 1–2 μm (Belmont and Bruce, 1994), but there is always the question of buffer-induced conformational changes in chromatin structure.

Significantly, the selective immunogold staining of the HSR shown in Fig. 7 now demonstrates similar diameter chromonema fibers within cells fixed directly in formaldehyde without prior detergent permeabilization. These ultrastructural results therefore strongly suggest that the apparent fibrillar HSR substructure visualized by light microscopy in vivo corresponds to irregular, tightly packed folding of these chromonema fibers.

4. Detection of a 256 Lac Operator Array Targeted to a Specific Chromosomal Location and Visualization of Sister Chromatid Separation during Anaphase in Yeast Cells. Ideally, use of lac operator/repressor staining as an in situ tag for specific chromosomal locations could be coupled with targeting of the lac operator array to specific chromosomal locations by homologous recombination. Demonstration of the feasibility of this approach in budding yeast is presented in Fig. 8. A targeting vector (pAFS59) containing a 256 lac operator direct repeat and the LEU2 gene was integrated into *Saccharomyces cerevisiae* strain AFS34. Integration was targeted to the leu2-3,112 locus approximately 10 kb from the centromere of chromosomeIII and was verified by Southern blotting.

A GFP–lac repressor–NLS fusion protein under the control of the HIS3 promoter was used for detection. Optimal detection, as described above for CHO cells, required expression of the GFP–repressor protein at appropriate levels, which produced strong specific staining but weak background nuclear fluorescence. Fig. 8 *A* shows haploid cells in G1 with one spot per nucleus as expected for cells with unreplicated DNA. Fig. 8 *B* shows haploid cells undergoing anaphase. The individual spots seen in G1 now have separated into two spots, one in the mother cell and one in the daughter cell. Fig. 8 *C* shows haploid cells arrested with nocadazole in mitosis; one spot per cell is seen indicating that the centromeres of sister chromatids have maintained their attachments to each other during mitotic arrest. The stability of the lac operator direct repeats during mitosis was demonstrated by Southern blot analysis (data not shown).

These experiments demonstrate the feasibility of localizing specific chromosomal sites in living yeast cells.

5. Following the Position of a DNA Segment Over Time in Animal Cells Undergoing Mitosis. Initial experiments have demonstrated that multiple exposures of both CHO and yeast cells expressing the GFP–lac repressor fusion protein are possible without compromising the viability of the cells. Fig. 9 shows results from CHO cells with the A03 HSR that stably express the lac repressor–GFP fusion protein. A series of images were acquired of a specific cell. Fig. 9 *A* shows the first image of the series, 4 h before cell division; Fig. 9 *B* shows an image of the two daughter cells 2 h after cell division. 1-s exposures were acquired every 30 min; total exposure in this series was ~15 s, including extra exposures required for focusing.

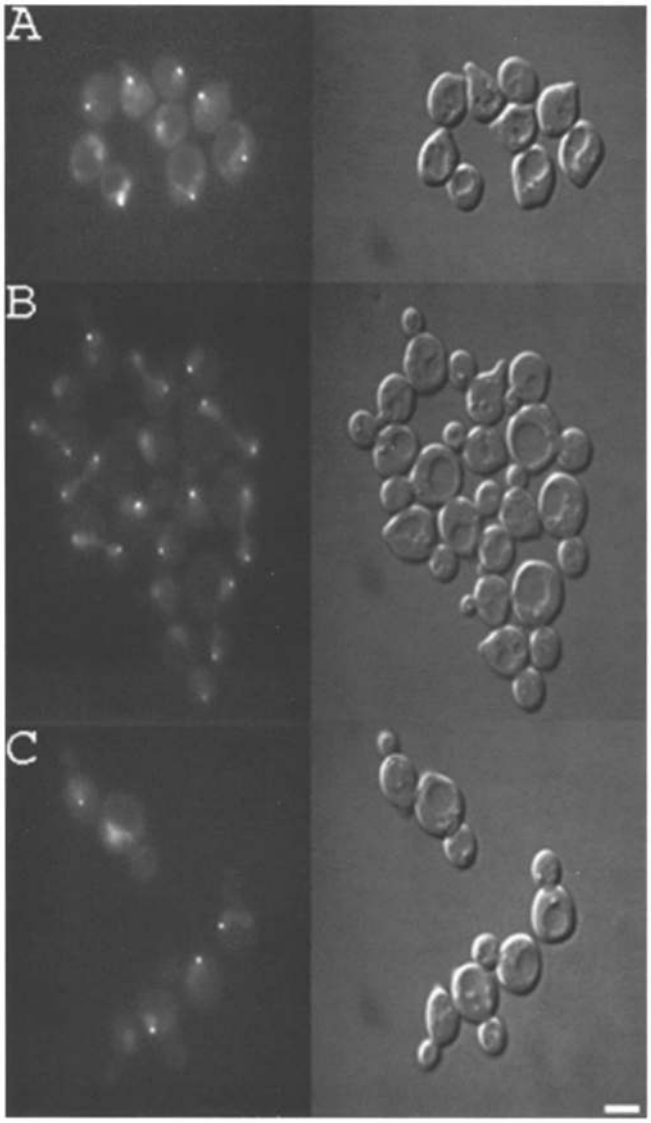

Figure 8. Live yeast cells tagged on chromosome III with lac operator repeats and expressing the GFP-lacI-NLS fusion. The left panels show GFP-lacI-NLS fluorescence and the right panels show Nomarski images of the yeast cells. (*A*) Cells arrested in α factor show a single staining spot. (*B*) 90 min after α factor release, cells have proceeded through anaphase showing separation of sister chromatids. (*C*) Cells released into nocodazole arrest in mitosis and block sister chromatid separation. Bar, 5 μm.

Discussion

Methodology

We have demonstrated the feasibility of using lac repressor staining of lac operator direct repeats for in situ localization of specific chromosome regions. Localization could be achieved by light microscopy using either staining of fixed cells or by direct in vivo imaging using a GFP–lac re-

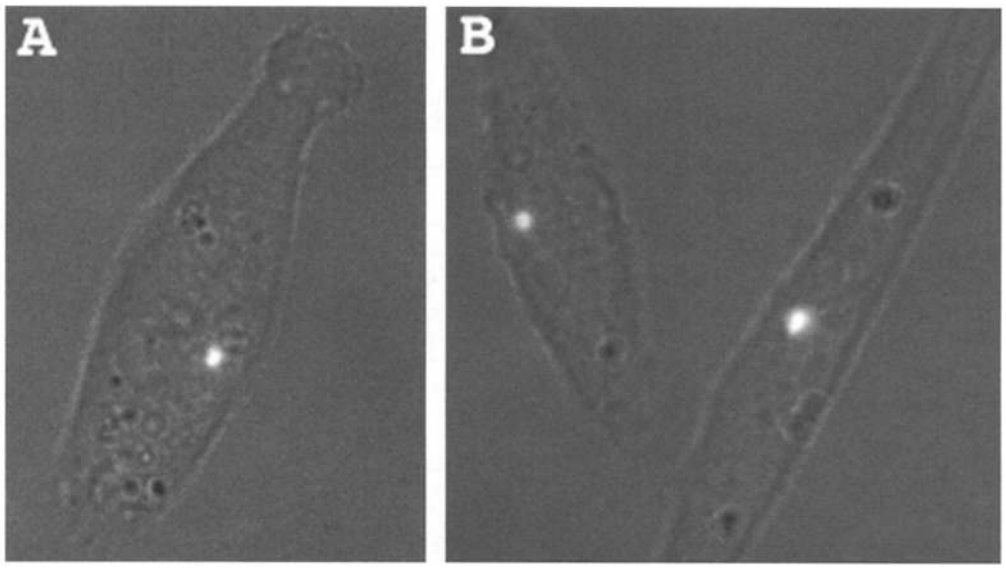

Figure 9. Extended in vivo imaging of GFP–repressor in CHO cells. Log phase A03 cells (see Fig. 5, text) stably transformed with GFP–repressor were grown at 37°C on microscope stage. Images were collected every 30 min during observation. Transmitted light and GFP fluorescence images were blended to give combined images. (*A*) Cell 4 h before cell division. (*B*) Daughter cells 2 h after cell division.

pressor fusion protein. The ability to carry out extended in vivo imaging was demonstrated and the use of preembedding immunogold labeling methods allowed localization at the ultrastructural level using transmission electron microscopy.

The capability of in vivo imaging of amplified chromosome regions allowed a direct comparison of in vivo interphase chromosome structure with that observed after treating cells according to a fluorescence in situ hybridization protocol. Our results demonstrate that the overall morphology and intranuclear location of amplified chromosome regions was preserved quite well by the FISH procedure using formaldehyde fixation. This comparison therefore validates the use of FISH methods as a general tool for examining the intranuclear positions of defined chromosome loci.

However, there was some blurring of fibrillar substructure seen after FISH or DNA denaturation procedures relative to that observed in vivo that was particularly noticeable in closely packed regions; this in vivo fibrillar substructure was preserved using immunostaining procedures in conjunction with lac operator/repressor staining. We attribute the lack of obvious fibrillar substructure within these closely packed regions to an artifactual chromosome decondensation produced during the DNA denaturation procedure. It is possible that alternative FISH protocols would have produced improved results. The availability of in vivo images of amplified chromosome regions provides an excellent tool for future optimization of in situ hybridization protocols using both light and electron microscopy.

In CHO cells, the sensitivity of the immunostaining method allowed detection of single integration sites containing multiple copies of the expression vector containing the lac operator repeats. In the EP1-4 CHO cell line, it was demonstrated that a single copy of the vector could be detected in vivo using the GFP–repressor fusion protein. In budding yeast, a single 256 lac operator repeat was easily detectable, suggesting that in this organism the detection sensitivity should allow detection of a smaller lac operator repeat size.

The ability to target via homologous recombination these lac operator arrays to specific chromosome locations in yeast will make this a powerful system for in vivo visualization of yeast chromosome structure and dynamics. Southern blot analysis indicates that these tandem lac operator arrays are stable in size through multiple mitotic cycles in both CHO cells and yeast. We suspect that this methodology will be generally applicable to a wide range of systems, which may allow analysis of specific chromosomal loci in transgenic animals. In *Drosophila melanogaster*, a 32 copy lac operator repeat has been stable in size, based on Southern blot analysis, for more than three years, which is equivalent to greater than 75 meiotic cycles and a much larger number of mitotic cycles; work now in progress has demonstrated the stability of the full 256 copy in Drosophila at least for several months (Sudlow, G., C. Robinett, C. Tolerico, A. Belmont, unpublished data).

In summary, this new method of in situ localization of specific chromosome regions using lac operator–repressor staining presents significant advantages for analysis of large-scale chromatin organization, particularly in its potential for visualizing in vivo chromosome dynamics and for higher resolution analysis of chromatin ultrastructure. Future development of this methodology should allow direct in vivo incorporation of lac repressor labeled with tags for electron microscopy localization, eliminating the need for immunostaining and further improving high resolution analysis of nuclear and chromosome ultrastructure.

Currently, a disadvantage of this methodology is its reliance on artificial constructs and the difficulty of multiple labeling. Conventional in situ hybridization at both the light and electron microscopy levels will therefore serve as a complementary and necessary tool, particularly for allowing comparisons with native chromosome structure and behavior. In the future, the use of other operator–repressor combinations in addition to lac, as well as operator arrays of variable size, may allow multiple labeling schemes, extending the range of applications of this technology, particularly when combined with targeting of these operator arrays to specific chomosomal sites.

Confirmation of Chromonema Fibers as a Basic Unit of Large-Scale Chromatin Folding

As described in the introduction, previous work described

~100-nm "chromonema" fibers within interphase nuclei as a basic unit of large-scale chromatin organization (Belmont et al., 1989; Belmont and Bruce, 1994); depending on cell cycle position, the actual predominant fiber diameter varied from 80–130 nm. In contrast, experiments using fluorescence in situ hybridization with probes that "paint" an entire chromosome or chromosome segment have visualized compact chromosome domains but have not recognized any distinct, fibrillar substructure (Cremer et al., 1993). Moreover, based on the statistical distribution of distances between chromosomal sites, measured using in situ hybridization, a random walk model for the folding of chromatin over a size scale of 100–1,000 kb and a looping over a 1,000-kb and larger size scale has been proposed (van den Engh et al., 1992; Yokota et al., 1995).

Using the lac repressor–operator staining methodology, we have visualized clear examples of extended fibrillar staining by light microscopy in living cells. At the same time, we have visualized what appears to be a fibrillar substructure within more compactly folded HSRs. Based on the estimated HSR sizes, this fibrillar staining corresponds to large-scale chromatin folding well above the 30-nm chromatin fiber in packing ratio. We also have demonstrated that previous failures to appreciate large-scale chromatin substructure within chromosome domains are consistent with structural perturbations in chromatin structure resulting from a standard in situ hybridization procedure. Although regions of extended fibers could still be visualized by in situ protocols, in regions where these fibers were tightly folded, the blurring occurring after DNA denaturation obscured the underlying fibrillar substructure. Therefore, appreciation of the underlying fibrillar substructure by in situ hybridization would normally require the appropriate size probes to chromosome regions forming extended fibers, rather than the usual tightly folded pattern. Based on our serial section analysis of G1 CHO nuclei, these extended regions are relatively rare (Belmont and Bruce, 1994).

Similarly, immunogold lac repressor staining of formaldehyde fixed cells revealed these HSRs were formed by large-scale chromatin folding with underlying fibrillar components well above 30-nm diameter. In thicker sections, extended fibrillar regions were visualized, with component fibers in the ~100-nm diameter range, consistent with our previous EM studies.

Because of the variable HSR size in the PDC cells used in this work, an exact estimation of the compaction ratio for these fibers is not yet possible. However, a packing ratio of 10,000:1 or greater for metaphase chromosomes, together with the ~0.5-μm or larger size of the PDC HSRs within metaphase chromosomes versus the estimated interphase length of tens of μm, predicts a packing ratio of these chromonema fibers on the order of several 100s–1,000s to 1. Work is now in progress to estimate the compaction ratio of these fibers more accurately using cell clones containing HSRs of fixed size.

What had not been absolutely certain in our previous studies of large-scale chromatin organization was whether the chromonema fibers we visualized were: (*a*) present in cells before extraction in polyamine buffer, (*b*) due to continuous, linear folding of a single contiguous DNA sequence versus a result of coincidental contact between several smaller condensed chromatin segments, or (*c*) typical of most chromosomal folding, given that for technical reasons the ability to trace these fibers by serial sectioning over 1–2 μm in length was limited to a small fraction of the total chromatin.

The results discussed above demonstrate that these chromonema fibers are not an artifact of a particular isolation buffer and do correspond to the organized folding into extended fibers of contiguous DNA sequence.

Application of this lac repressor staining technology should allow the detailed description of the unfolding/folding pathway for specific chromosome regions during the mitotic and interphase cell cycle. The capability of following the folding of chromosome regions of variable size should help to elucidate basic structural motifs underlying chromosome condensation and decondensation. Future development of this technology should allow direct visualization of the higher order chromatin folding of specific chromatin domains.

We thank Dr. Joan Betz (Regis College) for providing the lac operator 8-mer direct repeat, Dr. Lawrence Chasin (Columbia University, New York) for CHO DG44 cells, Dr. Kathleen Matthews (Rice University) for her generous donation of purified lac repressor, and Stratagene for providing anti–lac repressor antibody. TEM was carried out at the Center for Electron Microscopy at the University of Illinois, Champaign-Urbana.

This work was supported by National Institutes of Health grant GM-42516 and National Science Foundation grant DIR-8907921 to A. Belmont.

Received for publication 28 August 1996 and in revised form 17 October 1996.

References

Adolph, K.W. 1980. Organization of chromosomes in mitotic HeLa cells. *Exp. Cell Res.* 125: 95–103.

Agard, D.A., Y. Hiraoka, P. Shaw, and J.W. Sedat. 1989. Fluorescence microscopy in three dimensions. *Methods Cell Biol.* 30:353–377.

Alberts, B., D. Bray, J. Lewis, M. Raff, K. Roberts, and J.D. Watson. 1994. Molecular Biology of the Cell. Garland Publishing, Inc., New York. 335–399.

Belmont, A.S., and K. Bruce. 1994. Visualization of G1 chromosomes—a folded, twisted, supercoiled chromonema model of interphase chromatid structure. *J. Cell Biol.* 127:287–302.

Belmont, A.S., J.W. Sedat, and D.A. Agard. 1987. A three-dimensional approach to mitotic chromosome structure: evidence for a complex hierarchical organization. *J. Cell Biol.* 105:77–92.

Belmont, A.S., M.B. Braunfeld, J.W. Sedat, and D.A. Agard. 1989. Large-scale chromatin structural domains within mitotic and interphase chromosomes in vivo and in vitro. *Chromosoma.* 98:129–143.

Belmont, A.S., Y. Zhai, and A. Thilenius. 1993. Lamin B distribution and association with peripheral chromatin revealed by optical sectioning and electron microscopy tomography. *J. Cell Biol.* 123:1671–1685.

Boggs, S.S., R.G. Gregg, N. Borenstein, and O. Smithies. 1986. Efficient transformation and frequent single-site, single copy insertion of DNA can be obtained in mouse erythroleukemia cells transformed by electroporation. *Exp. Hematol.* 14:988–994.

Boy de la Tour, E., and U.K. Laemmli. 1988. The metaphase scaffold is helically folded: sister chromatids have predominately opposite helical handedness. *Cell.* 55:937–944.

Brown, M., J. Figge, U. Hansen, C. Wright, K.-T. Jeang, G. Khoury, D.M. Livingston, and T.M. Roberts. 1987. Lac repressor can regulate expression from a hybrid SV40 early promoter containing a lac operator in animal cells. *Cell.* 49:603–612.

Chao, M.V., H.G. Martinson, and J.D. Gralla. 1980. Lac operator nucleosomes. 2. lac nucleosomes can change conformation to strengthen binding by lac repressor. *Biochemistry.* 19:3260–3269.

Chen, C., and H. Okayama. 1987. High-efficiency transformation of mammalian cells by plasmid DNA. *Mol. Cell Biol.* 7:2745–2752.

Chen, J., and K.S. Matthews. 1992. Deletion of lactose repressor carboxyl-terminal domain affects tetramer formation. *J. Biol. Chem.* 267:13843–13850.

Cremer, T., A. Kurz, R. Zirbel, S. Dietzel, B. Rinke, E. Schrock, M.R. Speicher, U. Mathieu, A. Jauch, P. Emmerich, et al. 1993. Role of chromosome territories in the functional compartmentalization of the cell nucleus. *In* Cold Spring Harbor Symposia on Quantitative Biology. Cold Spring Harbor Lab-

oratory Press, Cold Spring Harbor, NY. 777–792.
Dancher, G. 1981. Localization of gold in biological tissue. A photochemical method for light and electron microscopy. *Histochemistry.* 71:81–88.
Delidakis, C., C. Swimmer, and F.C. Kafatos. 1989. Gene amplification: an example of genome rearrangement. *Curr. Opin. Cell Biol.* 1:488–496.
Fieck, A., D.L. Wyborski, and J.M. Short. 1992. Modifications of the E. coli Lac repressor for expression in eukaryotic cells: effects of nuclear signal sequences on protein activity and nuclear accumulation. *Nucleic Acids Res.* 20: 1785–1791.
Helm, R., A.B. Cubitt, and R.Y. Tsien. 1995. Improved green fluorescence. *Nature (Lond.).* 373:663–664.
Hiraoka, Y., J.R. Swedlow, M.R. Paddy, D.A. Agard, and J.W. Sedat. 1991. Three-dimensional multiple-wavelength fluorescence microscopy for the structural analysis of biological phenomena. *Semin. Cell Biol.* 2:153–165.
Hu, M.C.-T., and N. Davidson. 1987. The inducible lac operator-repressor system is functional in mammalian cells. *Cell.* 48:555–566.
Lawrence, J.B., R.H. Singer, and J.A. McNeil. 1990. Interphase and metaphase resolution of different distances within the human dystrophin gene. *Science (Wash. DC).* 249:928–932.
Manuelidas, L. 1985. Individual interphase chromosome domains revealed by in situ hybridization. *Hum. Genet.* 71:288–293.
Marsden, M.P.F., and U.K. Laemmli. 1979. Metaphase chromosome structure: evidence for a radial loop model. *Cell.* 17:849–858.
Miller, J.H., and W.A. Reznikoff. 1980. The Operon. Cold Spring Harbor Laboratory, Cold Spring Harbor, New York. 177–220.
O'Keefe, R.T., S.C. Henderson, and D.L. Spector. 1992. Dynamic organization of DNA replication in mammalian cell nuclei: spatially and temporally defined replication of chromosome-specific α-satellite DNA sequences. *J. Cell Biol.* 116:1095–1110.
Paulson, J.R., and U.K. Laemmli. 1977. The structure of histone depleted chromosomes. *Cell.* 12:817–828.
Peii, T., and J.S. Lim. 1982. Adaptive filtering for image enhancement. *Opt. Eng.* 21:108–112.
Pixton, J., and A.S. Belmont. 1996. NewVision: a program for interactive navigation and analysis of muliple 3-D data sets using coordinated virtual cameras. *J. Struct. Biol.* 116:77–85.
Rattner, J.B., and C.C. Lin. 1985. Radial loops and helical coils coexist in metaphase chromosomes. *Cell.* 42:291–296.
Sasmor, H.M., and J.L. Betz. 1990. Specific binding of lac repressor to linear versus circular polyoperator molecules. *Biochemistry.* 29:9023–9028.
Sikorski, R.S., and P. Hieter. 1989. A system of shuttle vectors and yeast host strains designed for efficient manipulation of DNA in Saccharomyces cerevisiae. *Genetics.* 122:19–27.
Subramani, S., R. Mulligan, and P. Berg. 1981. Expression of the mouse dihydrofolate reductase complementary deoxyribonucleic acid in simian virus 40 vectors. *Mol. Cell. Biol.* 1:854–864.
Tobey, R.A., N. Oishi, and H.A. Crissman. 1990. Cell cycle synchronization: reversible induction of G2 synchrony in cultured rodent and human diploid fibroblasts. *Proc. Natl. Acad. Sci. USA.* 87:5104–5108.
Trask, B.J. 1991. DNA sequence localization in metaphase and interphase cells by fluorescence in situ hybridization. *In* Functional Organization of the Nucleus: A Laboratory Guide. Academic Press, Inc., London. 4–32.
Urlaub, G., P.G. Mitchell, E. Kas, L.A. Chasin, V.L. Funanage, T.T. Myoda, and J. Hamlin. 1986. Effect of gamma rays at the dihydrofolate reductase locus: deletions and inversions. *Som. Cell Molec. Genet.* 12:555–566.
van den Engh, G.J., R. Sachs, and B.J. Trask. 1992. Estimating genomic distance from DNA sequence location in cell nuclei by a random walk model. *Science (Wash. DC).* 257:1410–1412.
Yokota, H., G. Vandenengh, J.E. Hearst, R.K. Sachs, and B.J. Trask. 1995. Evidence for the organization of chromatin in megabase pair-sized loops arranged along a random walk path in the human G0/G1 interphase nucleus. *J. Cell Biol.* 130:1239–1249.